Ultrasonic Crack Monitoring Using SH Waves in extreme and inaccessible environments

F.B. CEGLA
Department of Mech. Engineering, Imperial College London, London SW7 2AZ, UK
Tel: +44 (0)207 594 7227, Fax: +44 (0)207 584 1560
f.cegla@imperial.ac.uk

Abstract

The development of SH waveguide probes that can work under extreme conditions (Temperature>500°C, radiation) has opened up the possibility to carry out ultrasonic monitoring using SH waves on plant components that cannot be inspected otherwise. The deployment of such monitoring devices can result in substantial economic benefit by continuously supplying information about the state of a critical plant component rather than only at periods of shut down, which can be years apart. SH waves are often impractical in manual NDT due to coupling issues; however when permanently installed the simplicity of their interaction with defects becomes very attractive. This paper presents different crack size monitoring techniques using SH waves and highlights their advantages and disadvantages. Simulated as well as experimental results for laboratory specimens are presented.

Keywords: Crack monitoring, Online monitoring, SH waves

1. Introduction

In the past SH waves have not been very widely used in ultrasonic applications. This is mainly due to the unavailability of SH wave transducers and the need for shear coupling between the transducer and the structure (except for EMATs). The coupling issues are particularly detrimental in scanning applications which are most commonly used in practice. While the practical pitfalls have limited the use of SH waves in standard (manual) NDT applications they possess several advantages that can be exploited in monitoring applications. For permanently installed systems coupling can be ensured at the point of installation and hence monitoring applications can exploit the advantages of SH waves. The main benefits of SH waves are that they do not mode convert at oblique incidence on free surfaces and their slow bulk velocity compared to compression waves allows testing at low frequencies with the same spatial resolution.

There are a few researchers who have already investigated the use of shear waves for crack sizing applications such as Baskaran [1] who reports on the development of the time of flight diffraction technique (TOFD) using shear waves for thin specimens. Kimoto et al. [2] have presented the use of an SH array to size surface breaking cracks and the earlier work by Rao et al. [3] used EMAT generated SH waves for TOFD of surface breaking cracks. However as shown by Chapman [4] the amplitude of the diffracted SH waves greatly depends on the orientation of the crack and it is the physics of the SH diffraction that makes crack monitoring using TOFD from the opposite side to the crack very difficult if not unfeasible.

In this paper Chapman's [4] analysis of SH wave diffraction at a crack will be recalled in order to highlight the problems encountered by this technique, then a further

crack monitoring strategy based on multi-skip imaging using an array will be presented. Finite element results showing the successful imaging of simulated cracks will also be presented.

2. Theory

2.1 SH wave diffraction at a crack

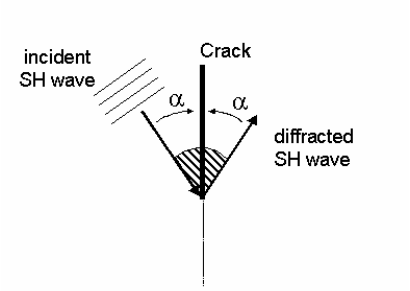

Figure 1. Illustration of geometry of SH wave diffraction at a crack that was considered by Chapman [4].

Figure 1 shows the geometry that was considered by Chapman [4] for the analysis of SH wave diffraction at a crack tip. He considered plane waves incident at angle α and found an expression for the amplitude of the diffracted wave at a receiver position that is symmetric to the incident plane wave with respect to the crack:

$$A_{SH} = -e^{i\pi/4} \frac{\cos^2\left(\frac{\alpha}{2}\right)}{2\pi\cos\alpha} \sqrt{\frac{\lambda}{R}} e^{ikR}. \tag{1}$$

Where α is the angle between the crack and the incident SH wave, λ is the wavelength of the incident SH wave, k is the wavenumber of the incident SH wave and R is the distance (radius) between the crack tip and the receiver.

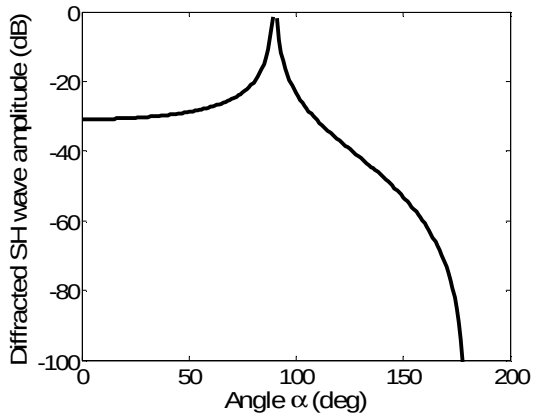

Figure 2. Diffracted wave amplitude at 50mm from the crack tip from a plane wave incident on a crack in a steel block.

Figure 2 shows the result of equation 1 plotted for a crack in a steel block at a receiver distance of 50mm from the crack tip. For low angles of incidence (i.e. when the

crack is surface breaking) the diffracted SH wave amplitude is equal to about -30dB of the incident wave. The diffracted wave amplitude increases up to an angle of 90 degrees where a singularity in the equation exists. At angles larger than 90 degrees, i.e. if the wave is incident from the far side with respect to the crack, the diffracted wave amplitude rapidly decreases. It drops to about -60 dB at an angle of 150 degrees and at 180 degrees the amplitude has dropped to about -100 dB.
The rapid decrease in amplitude of the tip diffracted wave at incidence angles from the far side means that detection of the crack tip diffraction is very difficult and unreliable from the far side. Thus SH wave TOFD is unsuitable for the job and one has to look for other robust techniques.

2.2 SH wave multi skip imaging

As shown by Chapman's [4] calculation and Kimoto's [2] experiments, crack tip diffraction is strong enough to size cracks if sender and receiver are located on the side where the crack breaks the surface. When the crack is placed on the other side however crack tip diffraction will be too small to be detected and one has to find other methods. One such method is multi-skip array imaging as described by Lorenz [5]. The multi skip approach makes use of the strong specular reflection from a crack and will not suffer from the low amplitude signals that are imposed by the physics of diffraction. The method is almost identical to synthetically focused phased array imaging however the indirect path via the backwall rather than the direct path is used in the image computation. Using this technique a much better vertical resolution is achieved and it is also possible to detect tip diffraction as the incident wave has been reflected from the back wall and is now approaching the crack from the correct side. SH waves lend themselves very well to this type of imaging as they do not undergo mode conversion at oblique incidence onto the backwall.

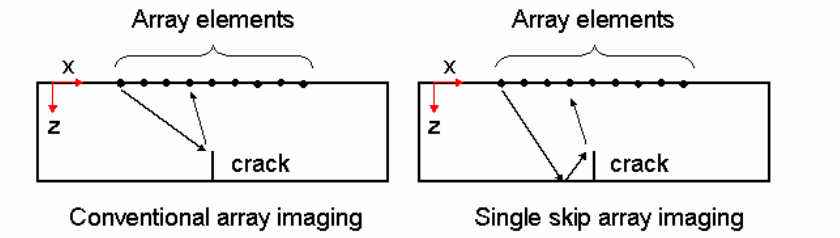

Figure 3. Illustration of conventional and multi skip (single skip shown) imaging using arrays.

Figure 3 compares the conventional array imaging approach with the multi skip (in this case single skip) approach. For simplicity a 2D approach is described here. It is immediately obvious that the difference between the two techniques lies in the processing of the results only. The techniques considered here are synthetically focused, meaning that the image processing is carried out after data acquisition by means of special algorithms. The data from all possible send and receive combinations of the elements within the array is assumed to be available so that processing using the total focusing method (TFM) as described by Homes et al. [6] can be carried out. The image can then be calculated from the acquired time traces:

$$I(x,z) = \left| \sum_{tx} \sum_{rx} S_{tx,rx} \left(\frac{d_{tx}}{v} + \frac{d_{rx}}{v} \right) \right| . \qquad (2)$$

Where d_{tx} is the distance between the image point and the transmitter location, d_{rx} is the distance between the image point and the receiver location, v is the bulk shear wave velocity in the material and $S_{tx,rx}$ is the signal received on receiver rx when sending on transmitter tx. Both d_{tx} and d_{rx} are functions of x and z.
For a conventional array the distances d_{tx} and d_{rx} are given by

$$d_{tx} = \sqrt{(x_{tx} - x)^2 + z^2} \quad and \quad d_{rx} = \sqrt{(x_{rx} - x)^2 + z^2} \tag{3}$$

where x_{tx} and x_{rx} are the positions of the transmitter and receiver respectively.
For the single skip imaging approach the only difference arises in the calculation of the distances of the transmitter from the imaging point as it is imposed that the wave has to be reflected from the backwall before reaching the imaging point. Equations 3 thus have to be adjusted to the following form:

$$d_{tx} = \sqrt{(x_{tx} - x)^2 + (t + (t - z))^2} \quad and \quad d_{rx} = \sqrt{(x_{rx} - x)^2 + z^2} \tag{4}$$

where t is the thickness of the specimen.

The technique was tested by FE simulations. Models of vertical notches of different lengths (3, 5, 10mm) were created in the ABAQUS explicit software [7]. For speed and simplicity a 2D acoustic model was used to represent the SH bulk waves in the simulation. The model component was 120mm wide and 20mm thick, it was given a density of 7932 kg/m^3 and a bulk wave velocity of 3260 m/s. An array of virtual point sources and receivers was placed on one side of the specimen. The array comprised 30 elements with inter-element spacing of 1mm. The first element was positioned in exactly the centre of the model specimen with element numbers increasing to the left. Notches were modeled by removing elements along a line. The elements were uniform and square of 0.1mm size. Figure 4 shows a sketch of the finite element model setup.

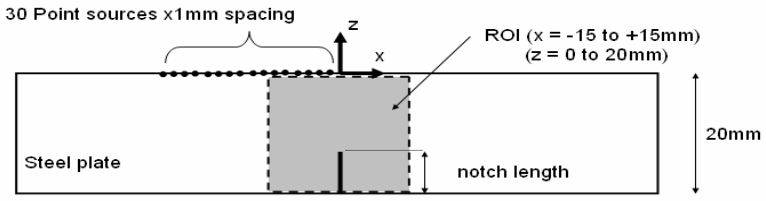

Figure 4. Finite element model used to simulate the single skip imaging of a vertical notch using SH waves.

Once the model was setup, it was run and time histories for each send/receive combination were acquired for the different notch sizes. 5 cycle Hanning windowed tonebursts at 2 MHz centre frequency were sent as the excitation signal. Data processing was performed as described in equations 2 and 4. The results of the finite element simulations are shown in figure 5. In the images the increase in notch size is clearly visible. On the right the actual computed image is shown while the picture on the left shows the 6dB contour line of the image on the right. The 6dB contour line is an indication of the size of the notch.

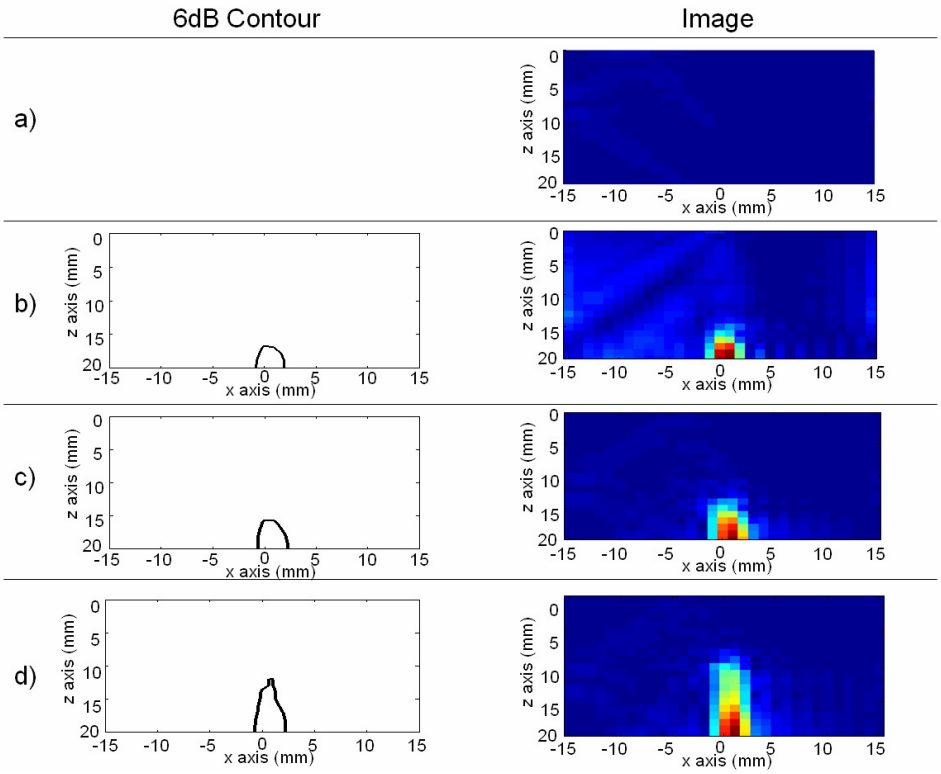

Figure 5. Image results obtained by processing the FE data using the single skip routine for a) no notch b) 3mm notch c) 5mm notch and d) 10mm notch.

3. EXPERIMENTS

Experiments were performed on a notched specimen in order to verify that the TOFD approach is only useful for surface breaking cracks. These results will be presented here. Experimental apparatus to perform single skip crack imaging is currently being built and results will be presented in the near future.

3.1 TOFD Setup

For the TOFD experiments a 15mm deep notch was cut into a 30mm mild steel plate. The steel block was then instrumented with 2 SH wave transducers with active area 1 by 15mm (polarized in the 15mm direction). The transducers were separated by 50mm and appropriately coupled to the specimen. One transducer was used as transmitter, the other as receiver. Due to the small width of the transducers ($w < \lambda$), the transducers can be assumed to act as a point sources which send and receive equally strong from/to all directions. Signals were sent and received by a purpose made function generator (Wavemaker Duett, Macro Design Ltd.) and displayed on a digital storage oscilloscope (LeCroy 9400A). From the storage oscilloscope the signals were downloaded to a PC in order to be stored and displayed. A 5cycle 2MHz Hanning windowed toneburst was used as the excitation signal. Three different signals were acquired. In one case the transducers were attached to the specimen far from the notch so that a reference measurement on the plate was possible. In the other two cases the transducers were attached on a position symmetric with respect to the notch on the surface breaking and the opposite side. A sketch of the setup is shown in figure 6.

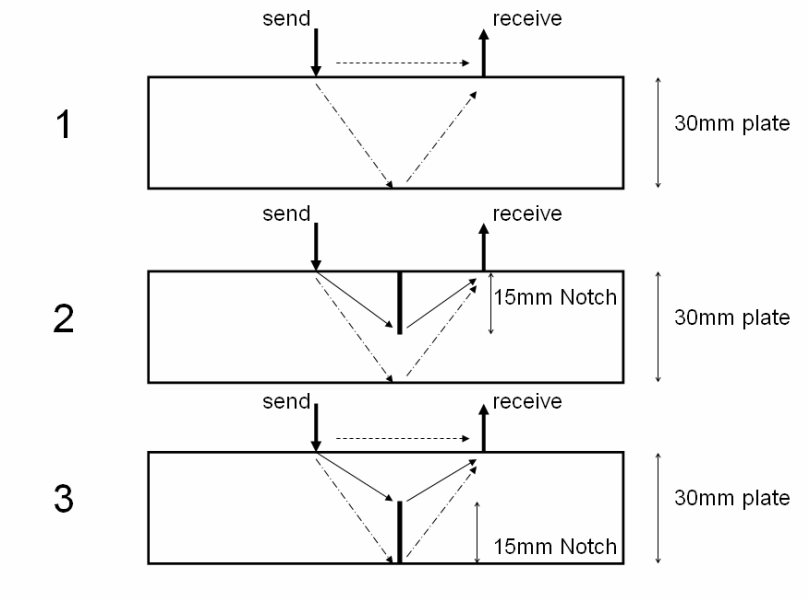

Figure 6. Sketch showing signal paths (--- surface signal, —crack tip diffracted signal, and -·-· backwall signal) and 3 experimental configurations to test SH wave TOFD data from a 15mm notch in a 30mm thick plate.

3.2 Results

The time traces that were received from the 3 configurations shown in figure 6 are plotted in figure 7. The two signals that are clearly visible in the first configuration are the signal that travels via the surface and the first reflection from the backwall that arrives x μs later. In the second configuration the surface signal has been blocked by the crack and the first signal that arrives is the weak crack tip diffraction followed by the backwall signal at the same arrival time as in configuration 1. In the third configuration the surface signal is apparent again and a strong backwall signal is also present, however the crack tip diffracted signal is not visible. The amplitude of the diffracted signal in this configuration is too weak to surpass the noise floor.

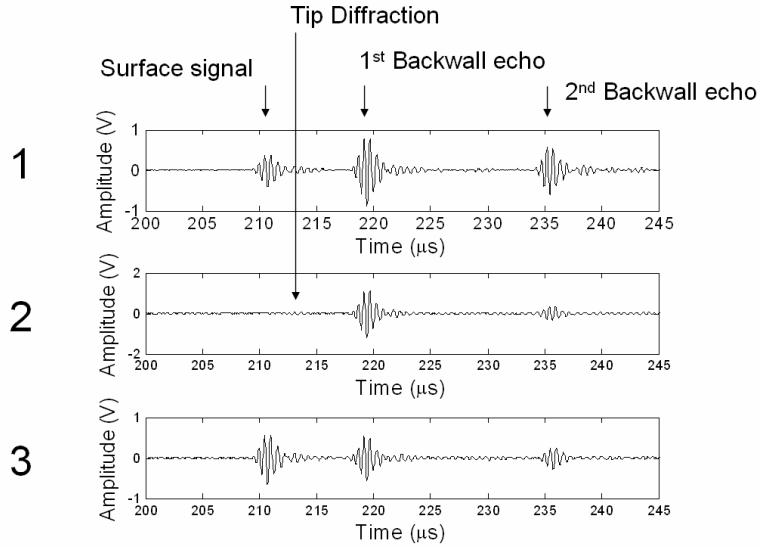

Figure 7. Time traces received from the three different experimental setups shown in figure 6: a) no notch b) surface breaking notch c) notch on the on the far side (relative to the transducers).

4. Conclusion

This work was motivated by the search for simple crack sizing techniques for permanently installable monitoring equipment. It was realized that the SH waves offer many desirable properties in permanently installable inspection scenarios without the practical issues around coupling that make it impractical for manual and scanning uses. Use of the TOFD technique using SH waves was investigated but it was found that it is only satisfactory for the sizing of surface breaking cracks due to the nature of the directivity of the tip diffracted wave. Predictions as well as experiments showed that the amplitudes of tip diffracted signals are too weak and difficult to detect when the cracks are on the far side. For this reason other techniques that do not rely on crack tip diffraction were investigated. It was found that a single skip imaging approach delivers potentially very good results. This was shown in a small FE study. Future experimental validation is being prepared.

Acknowledgements

This work was carried out as part of the TSEC programme KNOO with EPSRC funding under grant EP/C549465/1

References

1. G. Baskaran, G. Swamy, K. Balasubramaniam, C.V. Krishnamurthy, C. Lakshmana Rao,
   "Application of TOFD Techniques to thin sections using ESIT and PSCT", ", *in Review of Progress in Quantitative NDE*, Vol 24, edited by D.O. Thompson and D.E. Chimenti, NY, 2005, pp813-819.
2. K. Kimoto, S. Ueno, S. Hirose, "Image-based sizing of surface-breaking cracks by SH-wave array ultrasonic testing", Ultrasonics,Vol. 45, Issues 1-4, 2006, pp152-164.
3. B.P.C. Rao, G. Huebsch, H.-J. Salzburger, "Time-of-Flight Measurements with Shear Horizontal Waves.", 7th European Conference on Nondestructive Testing, Broendby, Denmark 1998. Vol. 3, ISBN: 87-986898-0-00, pp2979-2986.
4. R.K. Chapman, CEGB Report NW/SSD/RR/145/81, 1981, pp16-17
5. M. Lorenz, "Ultrasonic Imaging for the characterization of defects in steel components", Thesis Technishce Universiteit Delft, 1993, ISBN 90-9006160-6
6. C. Holmes, B.W. Drinkwater, P.D. Wilcox, "The post-processing of ultrasonic array data using the total focusing method", Insight - Journal of the British Institute of Non Destructive Testing, Vol. 46, Issue 11, 2004, pp677 – 680.
7. ABAQUS Reference Manuals, Version 6.5. ABAQUS Inc., Rising Sun Mills, 166 Valley Street, Providence, RI 02909-2499, USA, 2004.